ADSORPTION OF PCDD/F ON NITROGEN-DOPED BIOCHAR: A DFT-D STUDY

Xiong Shijian[1], Peng Yaqi[1],Tang Minghui[1], Lu Shengyong[1*], Li Xiaodong[1]

[1] State Key Laboratory of Clean Energy Utilization, Zhejiang University, Hangzhou, 310027, PR China, 11827072@zju.edu.cn;

Introduction

Polychlorinated dibenzo-p-dioxin and dibenzofurans (PCDD/F) are concerned with persistent organic pollutants due to extremely toxic and high carcinogenicity[1]. As a result, PCDD/F has a great threat to the environment and human health[2,] most from incineration. As for the removal of PCDD/F, adsorption[3] has been regarded as the most popular method to remove PCDD/F due to the advantages of the high removal efficiency (> 90%) and acceptable cost. Among PCDD/F congeners from incineration, 2,3,4,7,8-PeCDF[4,5] has been identified as the most contributor to international toxic equivalent (I-TEQ), with an international toxic factor of 0.5. Therefore, 2,3,4,7,8-PeCDF can be considered as the target molecule for the adsorption of PCDD/F.

Nowadays, nitrogen doping biochar is considered as the promising adsorbent for organic pollutants from incineration among carbon material due to environmentally friendly and effective adsorption[6]. Volatile organic compounds (VOCs) have been proven to be absorbed in nitrogen doping biochar effectively (585 mg/g)[7]. Moreover, as for the adsorption of SO_2[8], phenanthrene[9], and methanol[10], the effect of nitrogen doping has been reported. No research reports the adsorption of PCDD/F on nitrogen doping biochar. In the present study, the adsorption behavior of 2,3,4,7,8-PeCDF on nitrogen-doped biochar is investigated by density functional theory (DFT) and experiment. In addition, the electronic properties are analyzed by DFT.

Materials and methods

Considering the π-π stacking effect of the benzene ring, van der Walls interaction is introduced into the calculation system according to density functional theory based on dispersion correction (DFT-D3)[11-13]. The interactions between the valence electrons and the ionic core were described with the projected augmented wave (PAW) method. The electronic exchange-correlation potential was treated using the Perdew-Burke-Ernzerhof (PBE) functional[14,15]. A high energy cut-off of 400 eV was used for the plane-wave basis sets, with a convergence criterion set to 10^{-7} eV between two ionic steps for the self-consistency process. The Brillouin zone was sampled with a Monkhorst-Pack k-point grid of 2 ×2 × 1 for biochar surface due to the model size (17.2 Å ×17.2 Å× 18 Å). To determine the optimum adsorption sites and geometries, the 2,3,4,7,8-PeCDF molecule and each biochar surface allowed to relax unconstrainedly until residual forces on all atoms had reached 0.03 eV Å^{-1}. All calculations were carried out in Vienna Ab-initio Simulation Package (VASP) version 5.4.4. To obtain the energies of the 2,3,4,7,8-PeCDF molecule, the molecule was put into a space lattice of a = b= c= 15 Å to optimize.

Results and discussion

N-doped biochar

Firstly, according to X-ray photoelectron spectroscopy spectra of N 1s of nitrogen (N) doped biochar, graphitic nitrogen, pyridinic nitrogen, and pyrrolic nitrogen were proven on the surface of N-doped biochar. Then, the pristine and N-doped biochar surface with graphitic nitrogen, pyridinic nitrogen, and pyrrolic nitrogen was constructed. To investigated the electronic properties of the N-doped biochar surface, the charge density of pristine and N-doped biochar was illustrated in Figure 1. As compared with the pristine surface (Figure 1(a)), graphitic nitrogen, pyridinic nitrogen, and pyrrolic nitrogen doping all produce higher charge density and asymmetrical charge distribution. Moreover, the maximum charge density of the surface is the biochar with pyridinic N (0.668 eV), followed by the biochar with pyrrolic N atom (0.606 eV), the biochar with graphitic N atom (0.564 eV), pristine biochar (0.316 eV). The result implies the N doping increases the accumulation of electrons of the N atom. More specifically, the charge density of the N atom is two times that of the carbon atom on the graphitic N-doped biochar.
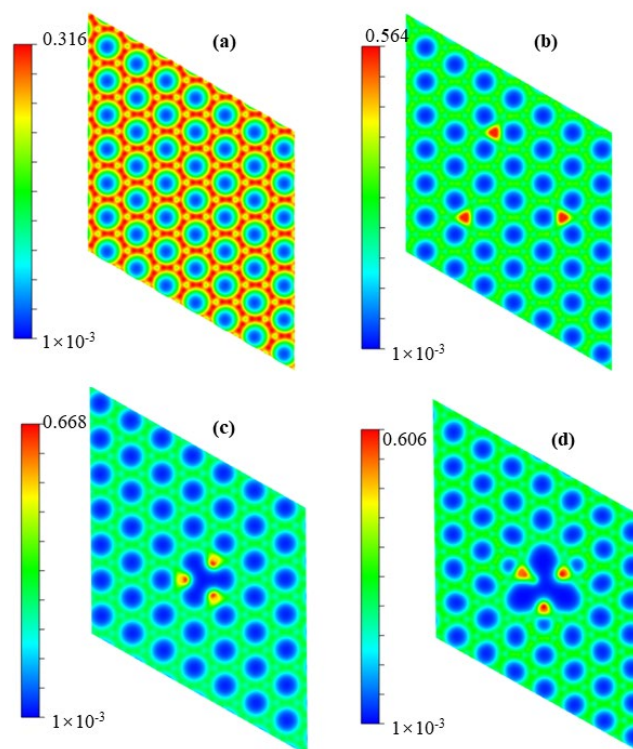
Figure 1. Charge density of pristine and N-doped biochar. Biochar without any N atom (a), with graphitic N (b), with a pyridinic N (c), and with pyrrolic N atom (d)

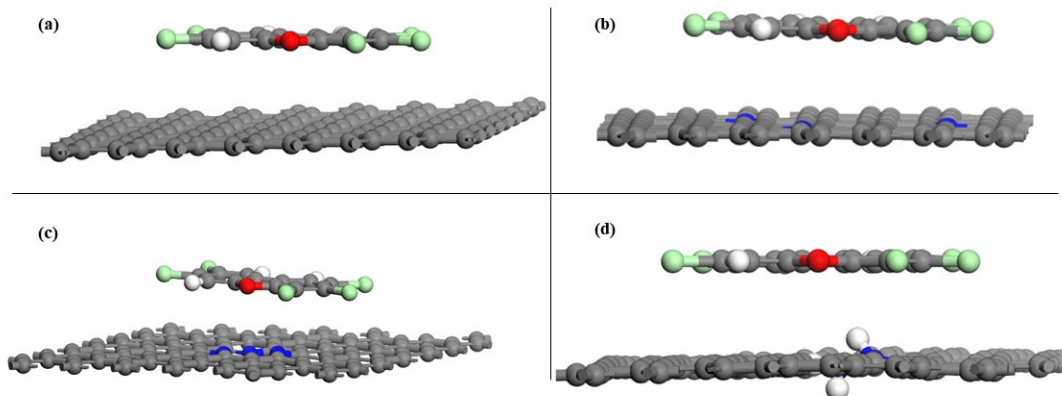**PeCDF adsorption on the N-doped biochar**

Figure 2. Optimized physisorption complex of PeCDF on biochar surface with and without N doping. Biochar without any N atom (a), with graphitic N (b), with a pyridinic N (c), and with pyrrolic N atom (d)

For the adsorption of PeCDF on the pristine biochar, various possible adsorption geometries were considered, including the hexagonal ring of PeCDF parallel and perpendicular to the biochar surface with chlorine site or oxygen site. It is founded that the two six-membered carbon rings of PeCDF parallel to the biochar surface are the most stable adsorption conformation. The adsorption energy between PeCDF and pristine biochar is -150.16 kJ•mol^{-1} (-1.564 eV), and the interaction distance is 3.593Å. The high adsorption energy and interaction for the physisorption complex of PeCDF on biochar surface indicate the strong physical adsorption of pristine biochar surface toward PeCDF via π-π stacking interaction.

Next, for the adsorption of PeCDF molecule on the N doped biochar, the optimized physisorption complex of PeCDF on biochar surface with and without N doping is illustrated in Figure 2. The adsorption energy between PeCDF and pristine and N doped biochar is presented in Table 1. For the graphitic N site adsorption, the adsorption

energy increases to -151.70 kJ•mol^{-1} from -150.16 kJ•mol^{-1} of pristine biochar. Moreover, the adsorption energy is -155.19 kJ•mol^{-1} and -155.56 kJ•mol^{-1} for pyridinic N and pyrrolic N site adsorption, respectively. It is found that N doping enhances the adsorption behavior of PeCDF on the biochar. In addition, the interaction distance decrease from 3.593 Å to 3.558 Å, 3.575 Å, 3.532 Å for graphitic N, pyridinic N, and pyrrolic N site adsorption, respectively. The smaller interaction distances imply the stronger interaction of PeCDF with N-doped biochar than the pristine biochar. The enhanced effect can attribute to the N doping increases the charge-transfer ability of biochar to PeCDF. Finally, the pyrrolic N site presents the highest adsorption energy and lowest interaction distance among the three N-doped sites. The result indicates that the optimized most stable site is the pyrrolic N site.

Table 1. Adsorption energy between PeCDF and pristine and N doped biochar

Species	$E_{ad}=E_{surface+PeCDF}-(E_{surface}+E_{PeCDF})$			
	$E_{surface+PeCDF}$(eV)	$E_{surface}$(eV)	E_{PeCDF}(eV)	E_{ads} (kJ•mol^{-1})
Graphite	-1046.26	-908.22	-136.47	-150.16
Graphitic-N	-1040.99	-902.94	-136.47	-151.70
Pyridinic-N	-1030.74	-892.65	-136.47	-155.19
Pyrrolic-N	-1021.23	-883.13	-136.47	-155.56

Electronic properties

To understand the improved adsorption capability of the biochar toward PeCDF upon the N doping, the total electronic density of state (DOS) of the stable adsorption site is calculated. As shown in Figure 3, the DOS of biochar near fermi level (energy = 0 eV) almost changed slightly after N doping. More specifically, the DOS of N-doped biochar is higher than that of pristine biochar in energy sbout -13 eV, 5 eV. Furthermore, the the obvious difference of biochar can be found in the total DOS result after the adsorption of PeCDF molecule. The result indicates that the strong interaction between biochar and PeCDF molecule. As for PeCDF adsorped on the pyridinic N-doped biochar, the DOS peak shifts to the left by 1 eV. In addition, among three N-doped adsorption configuration of PeCDF, the pyrrolic N-doped biochar display the highest peak. The result is consistant with the analysis of adsorption energy.
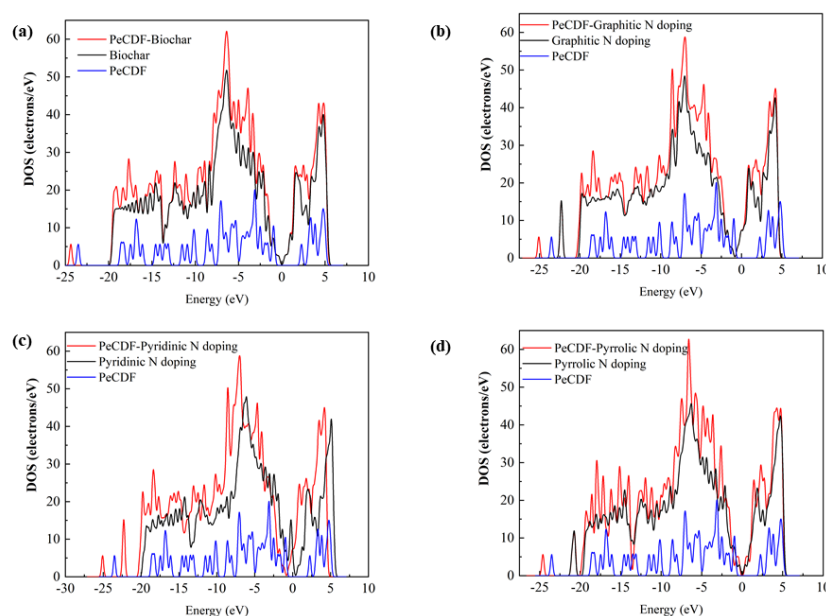

Figure 3. DOS of PeCDF on biochar surface with and without N doping. Biochar without any N atom (a), with graphitic N (b), with a pyridinic N (c), and with pyrrolic N atom (d)

References

1. Schecter.A, (2013).*Springer Science & Business Media*

2. Kulkarni, P. S., Crespo, J. G., & Afonso, C. A. (2008). *Environ. Int.*, 34(1), 139-153.

3. Chang, Y. M., Hung, C. Y., Chen, J. H., Chang, C. T., & Chen, C. H. (2009). *J. Hazard. Mater.* 161(2-3), 1436-1443.

4. Lin, X., Huang, Q., Chen, T., Li, X., Lu, S., Wu, H., ... & Wang, H. (2014). *Aerosol Air Qual. Res.* Research, 14(4), 1142-1151.

5. Ryu, J. Y., Mulholland, J. A., Kim, D. H., & Takeuchi, M. (2005). *Environ. Sci. Technol.*, 39(12), 4398-4406.

6. Wan, Z., Sun, Y., Tsang, D. C., Khan, E., Yip, A. C., Ng, Y. H., ... & Ok, Y. S. (2020). *Chem. Eng. J.*, 126136.

7. Lu, S., Huang, X., Tang, M., Peng, Y., Wang, S., & Makwarimba, C. P. (2021). *Environ Pollut.*, 284, 117113.

8. Qu, Z., Sun, F., Liu, X., Gao, J., Qie, Z., & Zhao, G. (2018). *Surf. Sci.*, 677, 78-82.

9. Wang, X., Guo, Z., Hu, Z., Ngo, H., Liang, S., & Zhang, J. (2020). *Sci Total Environ*, 733, 139267.

10. Ma, X., Li, L., Zeng, Z., Chen, R., Wang, C., Zhou, K., ... & Li, H. (2019). *Chem. Eng. J.*, 363, 49-56.

11. Hafner, J. (2008). *J. Comput. Chem.* 29(13), 2044-2078.

12 Georgieva, I., Trendafilova, N., Dodoff, N., & Kovacheva, D. (2017). *Spectrochimica Acta Part A.*, 176, 58-66.

13. Grimme, S., Antony, J., Ehrlich, S., & Krieg, H. (2010). *J. Chem. Phys.,* 132(15), 154104.

14. Wang, R., Zhang, D., & Liu, C. (2017). *Chemosphere*, 168, 18-24.

15. Zhang, H. P., Hou, J. L., Wang, Y., Tang, P. P., Zhang, Y. P., Lin, X. Y., ... & Tang, Y. (2017). *Chemosphere*, 185, 509-517.